

Carrier-Free Silibinin/Sorafenib Microparticles Alleviate Metabolic Dysfunction-Associated Steatotic Liver Disease by Modulating Fatty Acid Metabolism

Feifei Han^{1,*}, Haiping Wang^{1,2,*}, Li Wang¹, Limei Fan¹, Sibe Peng¹, Xiaoying Hou^{1,2}, Xiji Shu^{1,2}, Binlian Sun^{1,2}, Yuchen Liu^{1,2}

¹Cancer Institute, School of Medicine, Jiangnan University, Wuhan, Hubei, 430056, People's Republic of China; ²Hubei Key Laboratory of Cognitive and Affective Disorders, Jiangnan University, Wuhan, Hubei, 430056, People's Republic of China

*These authors contributed equally to this work

Correspondence: Yuchen Liu, Email yuchen.liu@jhun.edu.cn

Introduction: Metabolic dysfunction-associated steatotic liver disease (MASLD), characterized by excessive fat accumulation in the liver, is the most prevalent cause of chronic liver disease globally. The clinical use of pharmacological agents such as silibinin and sorafenib is limited due to poor water solubility, low bioavailability, and potential side effects, necessitating innovative therapeutic approaches.

Methods: In this study, we developed self-assembled, carrier-free microparticles of silibinin and sorafenib (SIL-SOR-MPs) using magnetic stirring and evaluated their therapeutic effects on MASLD both in vitro and in vivo.

Results: Compared to free SIL and free SOR, SIL-SOR-MPs significantly reduced lipid accumulation in HepG2 cells and effectively alleviated hepatic steatosis and liver damage in mice. Mechanistic investigations further showed that SIL-SOR-MPs more effectively down-regulated lipid synthesis genes and up-regulated genes involved in lipid oxidation.

Discussion: In summary, our study highlights that carrier-free SIL-SOR-MPs demonstrate the ability to reverse the progression of MASLD and present a promising therapeutic strategy.

Keywords: metabolic dysfunction-associated steatotic liver disease, silibinin, sorafenib, self-assembled carrier-free microparticles, fatty acid metabolism

Introduction

Metabolic dysfunction-associated steatotic liver disease (MASLD), is the most prevalent chronic liver condition globally, affecting approximately 38% of the population.^{1,2} Its incidence continues to rise due to changes in lifestyle and diet, making MASLD a growing public health concern.³ This progressive disease is characterized by excessive fat accumulation in the liver, progressing from simple steatosis to metabolic dysfunction-associated steatohepatitis (MASH), liver fibrosis, cirrhosis, and potentially hepatocellular carcinoma.⁴ As a multifactorial disease, MASLD is closely associated with metabolic disorders such as obesity, type 2 diabetes, hypertension, and hyperlipidemia.⁵ Its development is driven by mechanisms including lipid accumulation, insulin resistance, endoplasmic reticulum stress, oxidative stress, and activation of inflammation.^{6–8} Despite advancements in understanding MASLD pathogenesis, effective treatment remains a significant challenge. Rezdiffra was approved by the US Food and Drug Administration (FDA) for the treatment of MASH in March 2024. However, targeted therapies for the broader MASLD spectrum remain unavailable.⁹ The primary treatment strategy for MASLD relies on diet and lifestyle change interventions that are often difficult to implement and maintain.¹⁰ In clinical practice, the main medications used for MASLD include insulin sensitizers (eg, pioglitazone),

antioxidants (eg, vitamin E), and hepatoprotective drugs (eg, silibinin, ursodeoxycholic acid).¹¹ However, these drugs offer limited therapeutic benefits and often come with serious side effects due to low bioavailability and poor targeting. Furthermore, given the complex pathophysiology of MASLD, single target therapies have shown limited effectiveness. A combination of drugs targeting multiple pathways involved in MASLD may improve treatment outcome.

Silibinin possesses a range of pharmacological properties, including antioxidant, anti-inflammatory, antifibrotic effects, and the ability to modulate lipid metabolism.¹² It is widely used clinically to treat conditions such as liver damage, hepatitis, fatty liver, alcoholic or nonalcoholic liver diseases, and cirrhosis.¹³ Clinical studies have demonstrated that silibinin can effectively reduce liver enzyme levels, decrease fat accumulation, and improve liver function. Sorafenib primarily used to treat malignancies, including hepatocellular carcinoma and renal cell carcinoma, is a multi-target kinase inhibitor with additional anti-inflammatory and antifibrotic properties.¹⁴ Research by Jian et al found that low-dose sorafenib significantly alleviated the pathological phenotype of MASH by inducing mitochondrial uncoupling and activating AMP-activated protein kinase (AMPK) in both mice and rhesus monkey MASH models, without significant side effects.¹⁵ Therefore, low-dose sorafenib shows strong potential as a therapeutic option for managing MASLD and its associated complications.

Enhancing drug bioavailability and achieving effective concentration in target organs while minimizing systemic side effects is a major challenge in drug delivery. In recent years, nanotechnology has been widely applied to overcome the limitations of conventional delivery methods, particularly in terms of targeting and controlled release.¹⁶ However, traditional nano carriers, such as liposomes, polymers and similar substances have several drawbacks, including potential systemic toxicity, low drug loading capacity, and limited biocompatibility.¹⁷ To address these issues, carrier-free nanodrug systems have garnered significant attention due to their simpler preparation process and improved biosafety.¹⁸ Unlike traditional systems, carrier-free nanodrugs are composed entirely of one or more active drugs, which enhances pharmacokinetics, increasing drug loading capacity, and reducing toxicity.¹⁹ The self-assembly of two or more drugs into carrier-free particles, targeting multiple mechanisms involved in MASLD, offers a promising therapeutic approach. This strategy could provide a theoretical foundation and potential treatment for the clinical management of MASLD.

In this study, we utilized self-assembled, carrier-free drug delivery technology to design and develop dual-drug microparticles of silibinin and sorafenib (SIL-SOR-MPs). These self-assembled, carrier-free microparticles were engineered to enhance the solubility, stability, and targeting of both drugs, while also leveraging their synergistic effects for the treatment of MASLD (See [Scheme 1](#)).

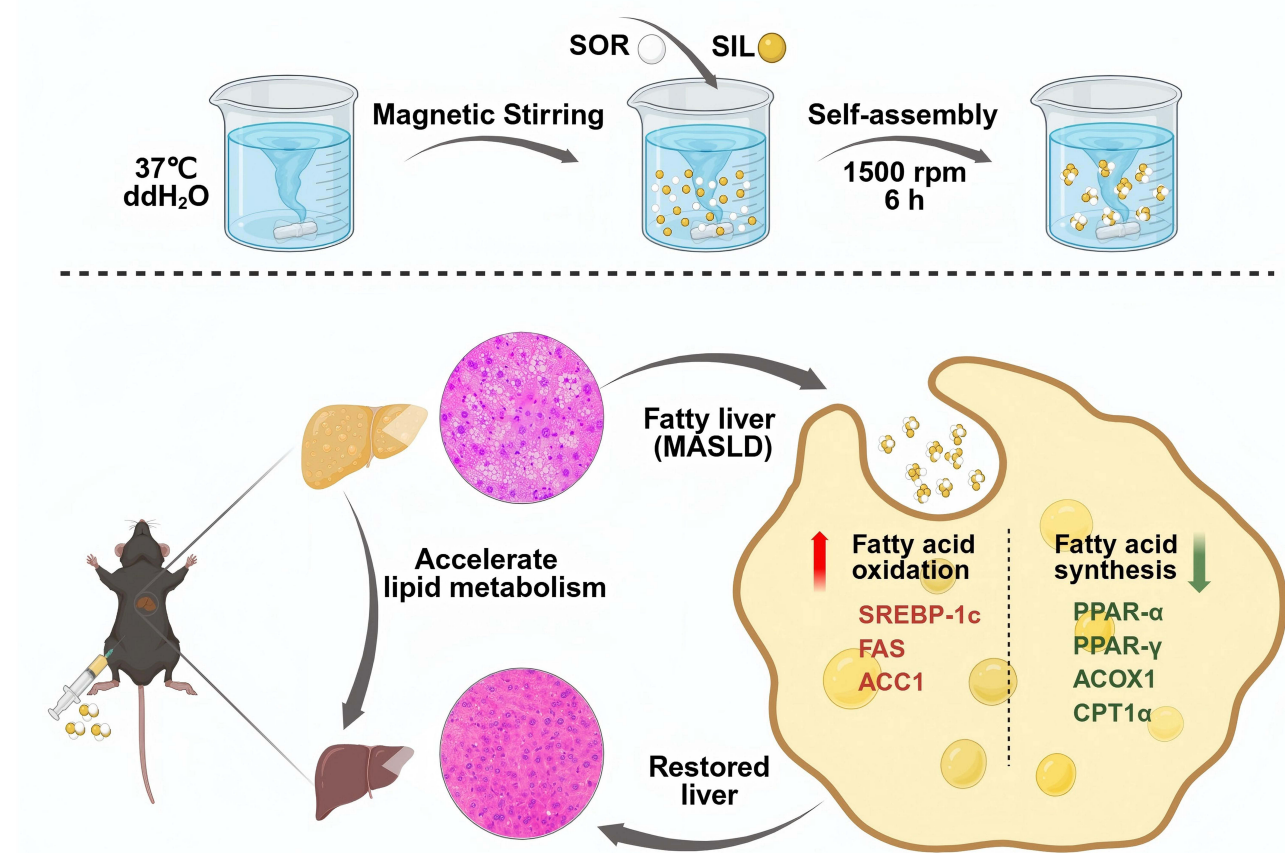
Material and Methods

Materials

Silibinin and sorafenib were purchased from Merck (Germany) and Aladdin (Shanghai, China), respectively. Dulbecco's modified eagle medium (DMEM), fetal bovine serum (FBS) and penicillin and streptomycin (PS) were from Gibco (USA). Sodium oleate (OA) and sodium palmitate (PA) were purchased from Macklin Biochemical Technology Co., Ltd (Shanghai, China). Oil red O staining kit and total cholesterol (TC) and triglyceride (TG) analytical kits were obtained from Jiancheng Bioengineering Institute (Nanjing, China). TRIzol reagent was provided by Ambion, USA First-strand cDNA synthesis kit and SYBR® Green qPCR Premix were acquired from Biology Biotechnology Co., Ltd (Wuhan, China). Both the dissolution and characterization of the particles were conducted using ultrapure water as the dispersion medium. All other chemical reagents used in this study were purchased from Sinopharm Chemical Reagent Co., Ltd (Beijing, China) and were of analytical grade.

Preparation and Characterization of SIL-SOR-MPs

Silibinin and sorafenib two-drug self-assembled microparticles were prepared by magnetic stirring method. Briefly, 10 mg/mL silibinin solution and 10 mg/mL sorafenib solution obtained by dissolving SIL and SOR in DMSO were dropped into the aqueous phase at a molar feed ratio of 3:1, respectively, and stirred homogeneously for 6 hours with magnetic stirring, then centrifuged to remove the organic and aqueous phases, and finally freeze dried to obtain the



Scheme 1 Schematic illustration of preparation of self-assembled, carrier-free silibinin/sorafenib microparticles and the treatment mechanism on MASLD.

carrier-free particle powders. Transmission electron microscopy (TEM, Hitachi JEM 1200EX, Japan) was used to characterize the morphology of SIL-SOR-MPs. The Malvern particle size analyzer was used to determine the size distribution and zeta potential of the prepared particles. All absorbance spectral data were recorded at room temperature using a UV/Vis spectrophotometer (PerkinElmer, USA).

Cell Culture and Treatments

Human hepatocellular carcinoma HepG2 cells were purchased from Cell Bank of Shanghai Institute of Biochemistry and Cell Biology, Chinese Academy of Sciences (Shanghai, China). HepG2 cells were cultured in DMEM medium supplemented with 10% FBS and 1% PS in an incubator at 37 °C, 5% CO₂, 95% humidity. To establish an in vitro cell model of MASLD, HepG2 cells were stimulated with DMEM medium containing free fat acid (FFA) (oleic acid: palmitic acid = 1000 μM: 500 μM) for 18 hours, which induced hepatocyte steatosis.²⁰ After 18 hours, the medium was discarded and the cells were treated with DMEM medium containing equal concentrations of free silibinin, free sorafenib and SIL-SOR-MPs for 24 hours, and the cells were stained with an Oil red O kit to visualize the lipid content. Cells control group was treated with DMEM medium. All cellular experiments were independently repeated at least 3 times (n≥3).

Cytotoxicity Assay

HepG2 cells were seeded in 96-well plates at a density of 1.5×10^5 cells/mL. After overnight incubation, the cells were treated with different concentration particles for 24 hours. Then, 10 μL of MTT (5 mg/mL) was added to each well and mixed. After incubation for 4 hours, the medium was discarded and 150 μL of DMSO was added to each well to dissolve the precipitate. The absorbance value of each well at 570 nm was measured using an automatic enzyme labeling

instrument (Thermo Fisher, USA). Cell viability was expressed as a percentage of the absorbance value of the treated cells to the control absorbance value.

Examination of Cellular Lipid Accumulation

Oil red O staining and Nile red staining were used to visualize cellular lipid accumulation. Briefly, FFA-stimulated HepG2 cells were dosed, fixed with 4% paraformaldehyde for 10 minutes at room temperature, and stained with Oil red O Staining Kit according to the manufacturer's instructions; or stained with configured 1 μ M Nile red solution for 30 minutes at room temperature protected from light, washed three times with PBS, and then stained the nucleus of the cells with DAPI for 10 minutes. The imaging was performed using an upright microscope (Olympus, Japan).

Animals and Treatments

All animal experiments were performed in accordance with the National Institutes of Health Guidelines for the Care and Use of Laboratory Animals and approved by the Institutional Animal Care and Use Committee of Jiangnan University (Wuhan, China, approval number: YXLL2023-005). Eight-week-old male C57BL/6 mice were purchased from Charles River (Beijing, China). All mice were placed in a standard environment with a light/dark cycle for 12 hours, free access to standard chow and water, and were acclimatized feeding for one week. To establish the MASLD mouse model, mice were fed on a normal diet (ND) and a high-fat diet (HFD) containing 60% caloric fat for 10 weeks. Subsequently, the high-fat diet-induced mice were randomly assigned to one of four treatment groups: the SIL group, the SOR group, the free SIL/SOR group (a non-formulated mixture of silibinin and sorafenib), and the SIL-SOR-MPs group. Treatments were administered over a 6-week period, during which MASLD model mice received intraperitoneal injections every other day with either 100 mg/kg of silibinin, 20 mg/kg of sorafenib, the free drug mixture, or microparticles containing equivalent doses of both silibinin and sorafenib. Mice in the normal diet control group received intraperitoneal injections of an equivalent volume of saline. Body weight was monitored and recorded prior to each administration.

In vivo Distribution Evaluation

To compare the enrichment of free SIL, free SOR, and SIL-SOR-MPs in mouse liver tissue, C57BL/6 mice were administered SIL-SOR-MPs or equimolar free SIL and SOR via intraperitoneal injection. At 2, 6, 12, 24 and 48 hours, mice were euthanized to dissect the liver tissues. Subsequent to tissue homogenization, quantify the specific absorption peaks of SIL and SOR in liver tissues utilizing a UV/Vis spectrophotometer. The content of SIL and SOR in tissues were calculated using standard curve.

Biochemical Analysis

To determine changes in lipids in vitro, lipids were extracted by ultrasonic disruption of cells, and total cholesterol (TC) and triglyceride (TG) levels in the cells were measured using an assay kit according to the manufacturers' protocol. To assess liver function in vivo, the changes in the levels of TC and TG in liver tissue were measured using the assay kit. For serum biochemical assess, the plasma was collected after centrifugation at 1150 g for 15 minutes at 4 °C, and the levels of alanine aminotransferase (ALT), aspartate aminotransferase (AST), TC, and TG were measured using a fully automated chemical analyzer (Rayto Life and Analytical Sciences, China).

Histological Staining

After all mice were executed, tissues of heart, liver, spleen, lung and kidney were dissected. All tissues were fixed with 4% paraformaldehyde for 48 hours, then dehydrated in an automatic dehydrator (Leica, German) and paraffin-embedded. Sections of 5 μ m were taken from the embedded tissues and then stained with hematoxylin and eosin (H&E). A portion of liver tissue samples preserved at -80 °C were embedded in optimal cutting temperature (OCT, Sakura, USA) and cut into 10- μ m-thick frozen sections for Oil red O staining using a frozen microtome (Leica, German) to evaluate hepatic fat accumulation. The tissue samples were analyzed under an upright microscope.

Quantitative Real-Time PCR Analysis

Total RNA was isolated and extracted using TRIzol reagent. The cDNA was reverse transcribed from RNA according to the cDNA Reverse Transcription Kit and then analyzed by real-time PCR on a Bio-Rad CFX Connect Real-Time PCR Detection System using the SYBR Green qPCR Mix kit. The thermal cycling protocol consisted of 5 minutes at 95 °C, 40 cycles of 10 seconds at 95 °C, and 60 seconds at 60 °C, complete with a melting curve at 60 °C to 95 °C. The relative mRNA expression was analyzed by the $2^{-\Delta\Delta CT}$ method and normalized to internal control β -actin. All primer sequences are shown in [Supplementary Tables S1](#) and [S2](#).

Statistical Analysis

All statistical analyses were based on a minimum of three independent biological replicates and are presented as mean \pm standard deviation (SD). Statistical analyses were performed using GraphPad prism 9 and statistical significance was assessed using Student's *t*-test or one-way ANOVA. Statistical significance was indicated by **p* < 0.05, ***p* < 0.001, and ****p* < 0.0001.

Results

Synthesis and Characterization of SIL-SOR-MPs

Carrier-free microparticles were synthesized by the self-assembly of the hydrophobic drugs silibinin and sorafenib at a molar feed ratio of 3:1 under magnetic stirring. The synthesis route is illustrated in [Figure 1A](#). Transmission electron microscopy (TEM) was used to examine the morphology of the microparticles. As shown in [Figure 1B](#), the SIL-SOR-MPs appeared to be relatively regular, exhibiting a uniform spherical shape. The particle size distribution and zeta potential of the microparticles were measured using dynamic light scattering (DLS). As shown in [Figure 1C](#), the average particle size was approximately 459 ± 4.06 nm. Additionally, the zeta potential of the SIL-SOR-MPs was measured at -23.6 mV ([Figure 1D](#)), which likely contributes to the prevention of particle aggregation and deposition, reduces protein adsorption, and prolongs blood circulation in vivo.²¹ This stability is inferred to arise from intermolecular interactions between silibinin and sorafenib. In order to explore the mechanism of self-assembly, we analyzed the UV/Vis spectral changes before and after particle formation. As shown in [Figure 1E](#), the characteristic peaks of the synthesized microparticles exhibited significant shifts compared to those of the individual drugs. We further examined the absorption spectrum of SIL-SOR-MPs in the presence and absence of NaCl and SDS.²² With increasing concentrations of NaCl, the absorption intensity progressively decreased ([Figure 1F](#)). Additionally, after co-incubation with the hydrophobic SDS, the spectral profile of the microparticles changed markedly ([Figure 1G](#)). These findings suggest that NaCl and SDS disrupt the electrostatic and hydrophobic interactions between the particle molecules, respectively. Based on these results, we propose that the self-assembly of silibinin and sorafenib is driven by intermolecular electrostatic and hydrophobic interactions.

SIL-SOR-MPs Effectively Attenuate Lipid Deposition in an in Vitro Cell Model of MASLD

An in vitro MASLD cell model was established using FFA-stimulated HepG2 to evaluate the effects of SIL-SOR-MPs on lipid deposition in hepatocytes. First, the cytotoxicity of the microparticles was assessed using MTT assay. As shown in [Figure 2A](#), co-incubation of SIL-SOR-MPs with HepG2 cells led to a concentration-dependent inhibition of cell viability. When the concentrations of silibinin and sorafenib in SIL-SOR-MPs were below 50 μ M and 10 μ M, respectively, the cell survival rate remained above 70%, indicating satisfactory biocompatibility of the particles. Next, HepG2 cells were treated with FFA alone or in combination with free silibinin, free sorafenib and SIL-SOR-MPs. [Figure 2B](#) and [C](#) show that FFA treatment significantly increased intracellular TC and TG levels. With both silibinin and sorafenib individually reduced TC and TG levels, SIL-SOR-MPs exhibited a more pronounced reduction in these lipid markers. Furthermore, as shown in [Figure 2D](#), Oil red O staining and Nile red staining consistently demonstrated that lipid droplet formation in HepG2 cells was reduced following treatment with silibinin, sorafenib, and most notably, SIL-SOR-MPs demonstrated the most potent inhibition of cytosolic lipid droplet accumulation induced by FFA exposure. To investigate the

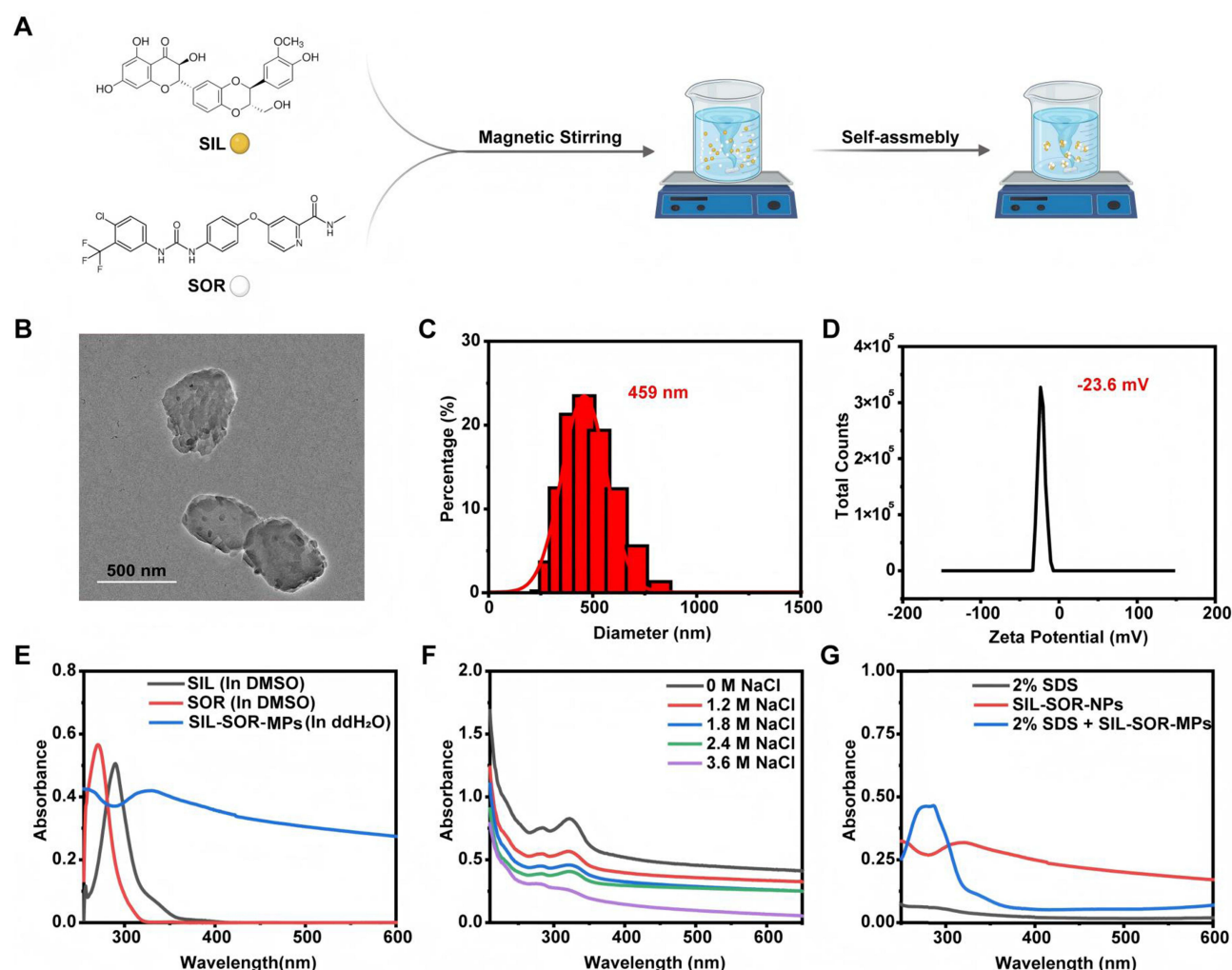


Figure 1 Preparation and characterization of SIL-SOR-MPs. **(A)** Schematic illustration of the synthesis process of SIL-SOR-MPs. **(B)** TEM image showing the morphology of SIL-SOR-MPs. **(C)** Particle size distribution of SIL-SOR-MPs as measured by dynamic light scattering. **(D)** Zeta potentials values of SIL-SOR-MPs, indicating the surface charge. **(E)** UV/Vis spectra of SIL, SOR and SIL-SOR-MPs in double distilled H₂O or DMSO, showing the characteristic absorption peaks. **(F)** UV/Vis spectra of SIL-SOR-MPs in varying concentrations of NaCl, illustrating the effect of electrostatic interactions on the particle absorption. **(G)** UV/Vis spectra comparing 2% SDS, SIL-SOR-MPs alone, SIL-SOR-MPs with 2% SDS, highlighting changes in spectral behavior upon interaction with SDS.

underlying mechanisms, the expression of key genes involved in fatty acid synthesis and oxidation was analyzed using qRT-PCR. As shown in **Figure 2E** and **F**, SIL-SOR-MPs significantly down-regulated the expression of sterol regulatory element binding protein-1c (*SREBP-1c*), fatty acid synthase (*FAS*), and acetyl-coenzyme A carboxylase1 (*ACC1*), while up-regulated the expression of peroxisome proliferator-activated receptor α (*PPAR-\alpha*), peroxisome proliferator-activated receptor γ (*PPAR-\gamma*) and carnitine palmitoyltransferase 1a (*CPT1a*) expression. These findings suggest that SIL-SOR-MPs may reduce lipid accumulation by modulating lipid metabolic reprogramming.

Biodistribution of SIL-SOR-MPs in C57BL/6 Mice

To assess the liver-targeting capacity of SIL-SOR-MPs, C57BL/6 mice were divided into two groups and administered either intraperitoneal injections of SIL-SOR-MPs or equimolar doses of free SIL/SOR. Liver samples were collected at various time points (2, 6, 12, 24 and 48 hours), homogenized, and analyzed to quantify drug levels using a UV/Vis spectrophotometer. As shown in **Figure 3A** and **B**, drug concentrations in the group treated with free SIL/SOR peaked at 6 hours and gradually decreased over time. In contrast, the group receiving SIL-SOR-MPs showed a steady increase in drug levels throughout the 48-hour period. Notably, at 48 hours post-administration, the hepatic concentrations of SIL and SOR in the SIL-SOR-MPs

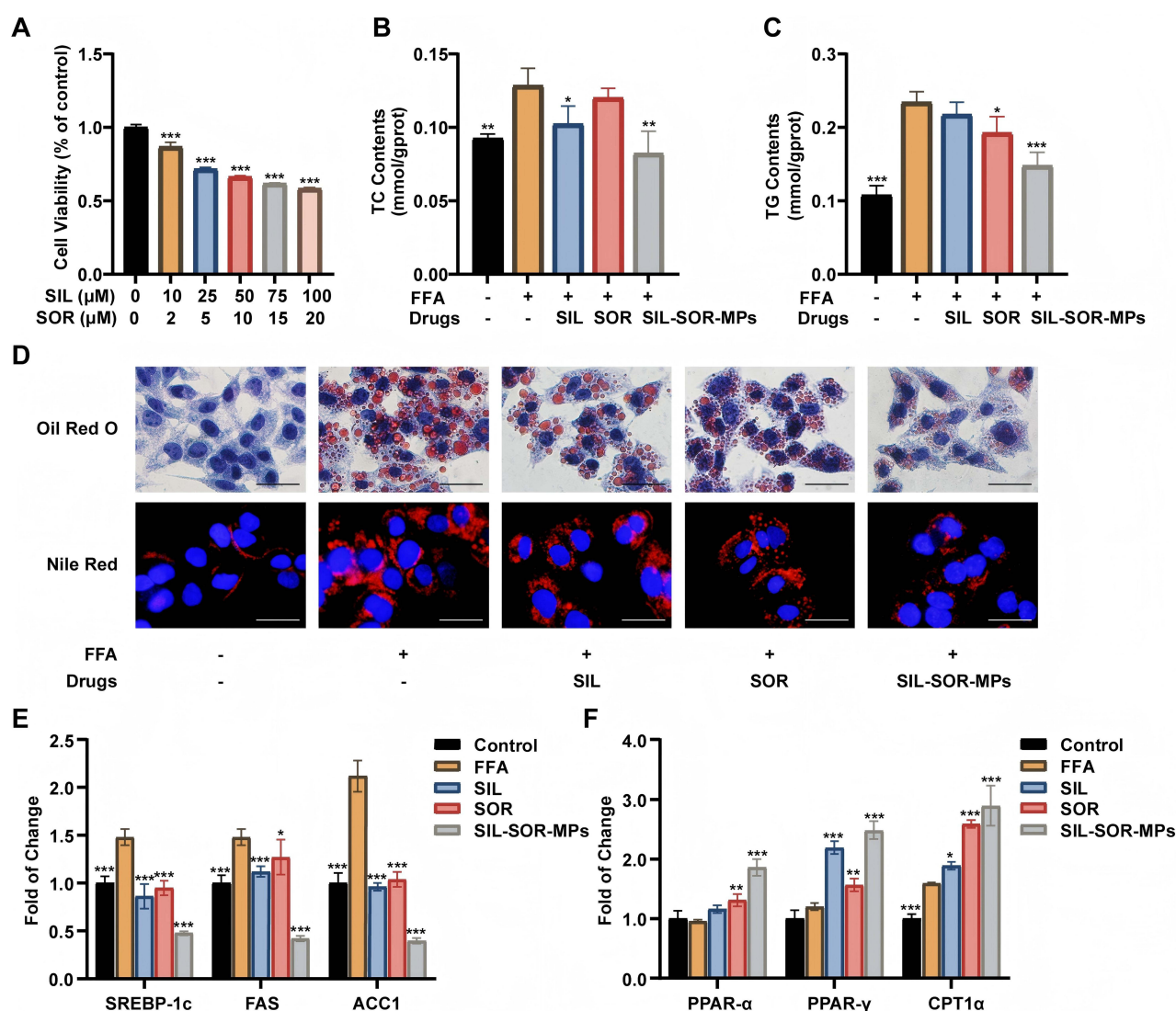


Figure 2 Cytotoxicity and lipid-lowering effects of SIL-SOR-MPs on HepG2 cells in vitro. **(A)** Cytotoxicity assessment of SIL-SOR-MPs in HepG2 cells. **(B)** Quantitative analysis of TC contents in cells. **(C)** Quantitative analysis of TG levels in cells. **(D)** Oil red O and Nile Red staining showing lipid accumulation in different treatment groups. **(E)** Quantitative analysis of fatty acid synthesis gene expression (*SREBP-1c*, *FAS*, *ACC1*). **(F)** Quantitative analysis of fatty acid oxidation gene expression (*PPAR-α*, *PPAR-γ*, *CPT1α*). * $P < 0.05$, ** $P < 0.001$, *** $P < 0.0001$ (FFA vs others). Scale bar: 20 μm .

group were 18.2-fold and 7.4-fold higher, respectively, compared to those in the free SIL/SOR group. These results demonstrate that SIL-SOR-MPs enhance hepatic drug accumulation and extend systemic circulation time.

SIL-SOR-MPs Inhibit the Progression of Steatosis in HFD Mice

To evaluate the in vivo efficacy of SIL-SOR-MPs, we used a high-fat diet (HFD)-fed C57BL/6 mouse model. After 10 weeks on the HFD, severe hepatic steatosis was induced, confirming the successful establishment of a MASLD model. Then, the mice were then randomized into four groups for drug treatments over a 6-week period, while continuing the HFD. The treatment protocol is shown in Figure 4A. Representative images of mice from each group were taken after the treatment (Figure 4B). The body weight was measured throughout the treatment phase. As shown in Figure 4C, mice in the HFD group gained significantly more weight compared to the other groups. However, mice treated with free SIL, free SOR, or free SIL/SOR showed a reduction in body weight, with the SIL-SOR-MPs treated group demonstrating the most substantial weight loss, comparable to mice on a standard chow diet. Analysis of liver weights (Figure 4D) revealed that the HFD group had significantly heavier livers than the normal-diet group. Treatments with free SIL, free SOR, free

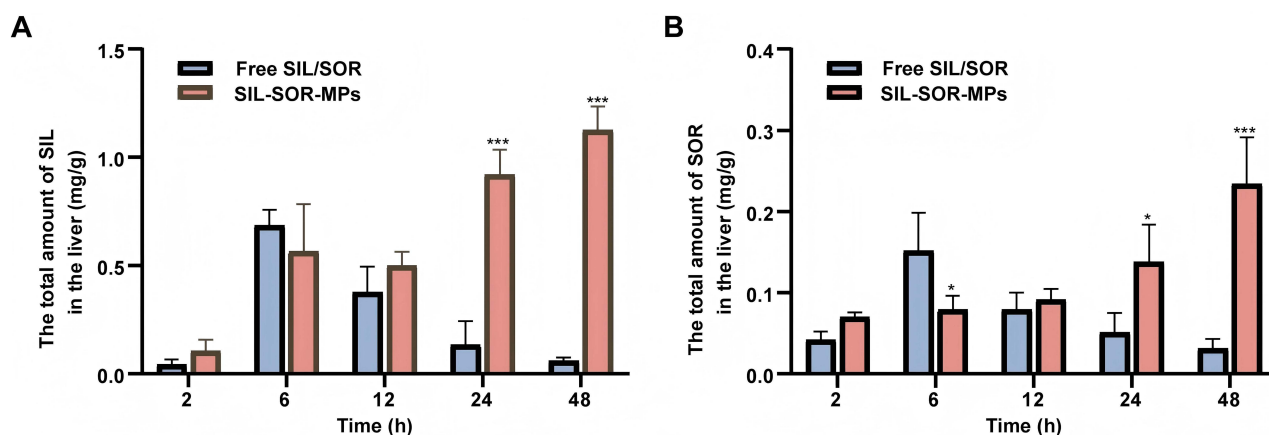


Figure 3 The distribution of SIL-SOR-MPs in the liver. Quantitative analysis was conducted to assess the distribution of SIL (A) and SOR (B) in mice following intraperitoneal injection. Drug content was measured in both the free SIL/SOR and SIL-SOR-MPs groups at 2, 6, 12, 24, and 48 hours post-administration. Each group consisted of 3 mice (n=3). * $p < 0.05$, *** $p < 0.0001$ (Free SIL/SOR vs SIL-SOR-MPs).

SIL/SOR, and SIL-SOR-MPs reduced liver weight in the MASLD mice, with SIL-SOR-MPs showing the most pronounced effect. Morphological examination of the livers at the end of the treatment period revealed substantial differences between the groups (Figure 4E). Livers from the normal-diet group were chocolate-colored, firm, and small, whereas those from the HFD model group were pale yellow, rough and considerably larger. All treatment groups showed some degree of improvement, with the livers of the SIL-SOR-MPs group being dark red, smaller in size, and almost fully restored to the appearance of livers from the normal-diet group. Histological analysis using H&E and Oil red O staining was performed on the liver tissues from all groups (Figure 4E). H&E staining showed that hepatocytes from mice on a normal diet were tightly packed and well organized. In contrast, hepatocytes from HFD mice were distorted and contained numerous droplet vacuoles. Treatment with free SIL, free SOR, free SIL/SOR alleviated lipid accumulation to some extent, but the livers of mice treated with SIL-SOR-MPs closely resembled those of normal-diet mice, demonstrating a significant reduction in fat accumulation. Oil red O staining further confirmed these findings, highlighting substantial lipid accumulation in the livers of HFD mice, while SIL-SOR-MPs treatment markedly reduced these accumulation, consistent with the H&E results.

SIL-SOR-MPs Regulate Lipid Metabolism During HFD Feeding

To investigate the therapeutic effects of various treatments groups on fatty liver in mice, we quantified TC and TG levels in both hepatic tissue and serum. As shown in Figure 5A and B, TC and TG levels in the livers of HFD-fed mice were significantly elevated compared to the normal-diet group. However, in the SIL-SOR-MPs group, these levels were substantially reduced, approaching those observed in normal mice. We also assessed the impact of the treatments on overall lipid profiles and liver function. Figure 5C–F show that serum levels of TC, TG, alanine aminotransferase (ALT) and aspartate aminotransferase (AST) were significantly higher in the model group than in the normal-diet group, indicating dyslipidemia and impaired liver function. At the end of the treatment period, the SIL-SOR-MPs group demonstrated the most effective reduction in HFD-induced elevated levels of TC, TG, AST and ALT, reflecting the best recovery among the treatment groups. These findings suggest that SIL-SOR-MPs provide strong protection against steatosis and liver injury.

To further explore the mechanism by which SIL-SOR-MPs reduce lipid accumulation in vivo, we examined the expression of key genes involved in lipid metabolism. As shown in Figure 5G, consistent with the in vivo results, the expression of lipid synthesis genes (*SREBP-1c*, *FAS*, *ACCI*) was significantly up-regulated in the HFD group, but most notably reversed in the SIL-SOR-MPs group. Additionally, microparticle treatment significantly upregulated the expression of genes related to fatty acid oxidation, including *PPAR-α*, *CPT1α*, and acyl coenzyme A oxidase 1 (*ACOX1*). In

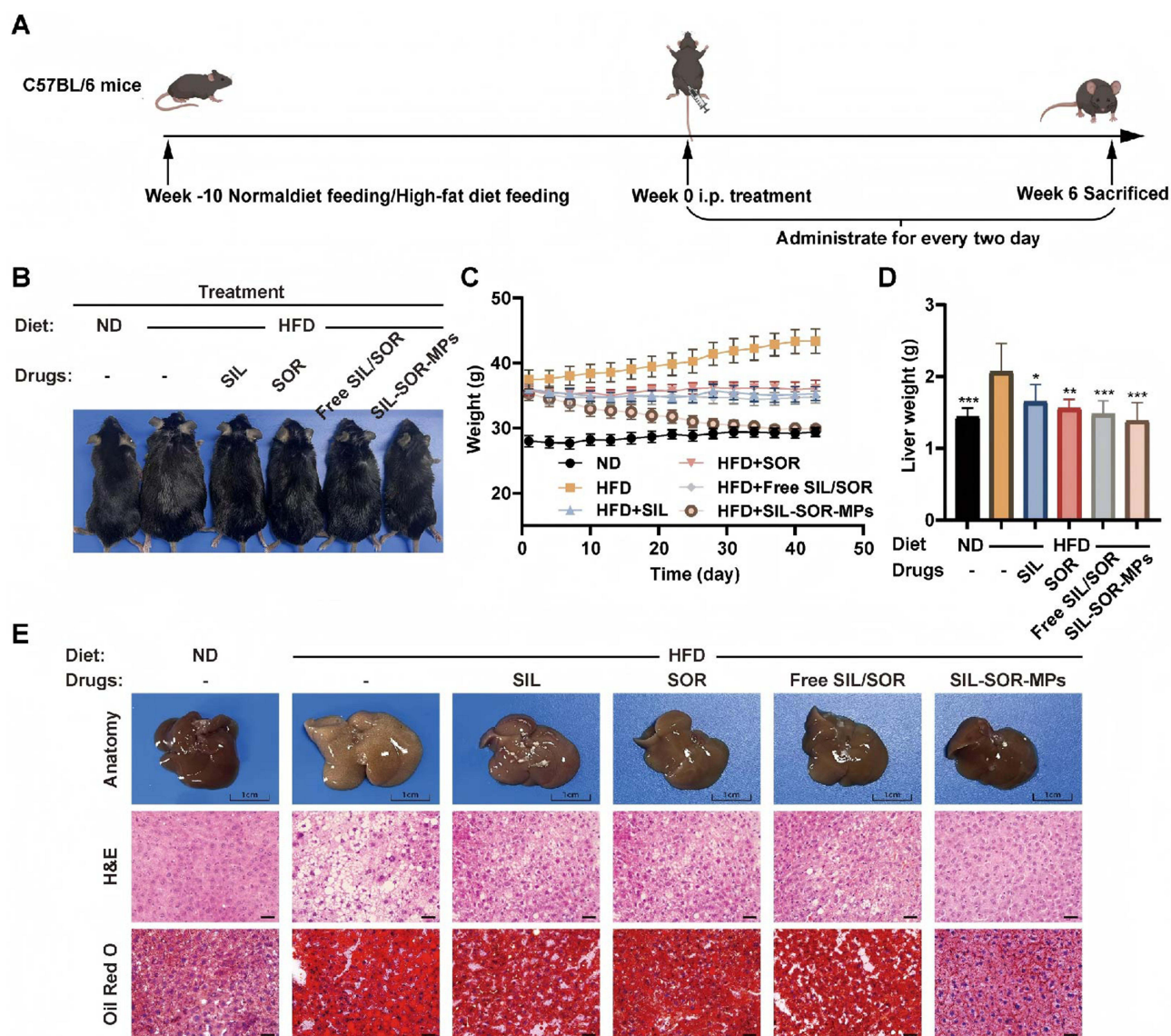


Figure 4 SIL-SOR-MPs inhibit HFD-induced MASLD progression. **(A)** Schematic representation of the animal experiment design. The drug treatments of the animals were divided into 6 groups: ND, HFD, HFD+SIL, HFD+SOR, HFD+Free SIL/SOR and HFD+SIL-SOR-MPs. **(B)** Photographs of MASLD mice following different treatment interventions. **(C)** Changes in body weight of mice throughout the treatment period. **(D)** Measurement of liver weight at the end point of experiments. **(E)** After 6 weeks of treatment, liver morphology (top panel), H&E staining (middle panel), and Oil red O staining (bottom panel) were analyzed for each group of mice. * $p < 0.05$, ** $p < 0.001$, *** $p < 0.0001$ (HFD vs others). ND: normal-diet, HFD: high-fat diet. Scale bar: 20 μ m, 400 \times magnification.

conclusion, SIL-SOR-MPs effectively reduce intrahepatic lipid deposition and improve lipid metabolism in HFD-fed mice, offering significant protection against MASLD-induced liver damage.

Biosafety Analysis of SIL-SOR-MPs

To evaluate the systemic toxicity of SIL-SOR-MPs in mice, major organs including the heart, spleen, lung and kidney were collected at the end of experiment for histological analysis. As shown in Figure 6, no significant pathological damage was observed in any of the organs from the treatment groups, demonstrating the excellent biocompatibility of the SIL-SOR-MPs. These results confirm their safety for therapeutic application.

Discussion

MASLD has become a significant global health challenge.²³ Its development is driven by the excessive accumulation of lipids in the liver, leading to impaired hepatocellular function.^{24,25} Over time, this lipid accumulation triggers oxidative

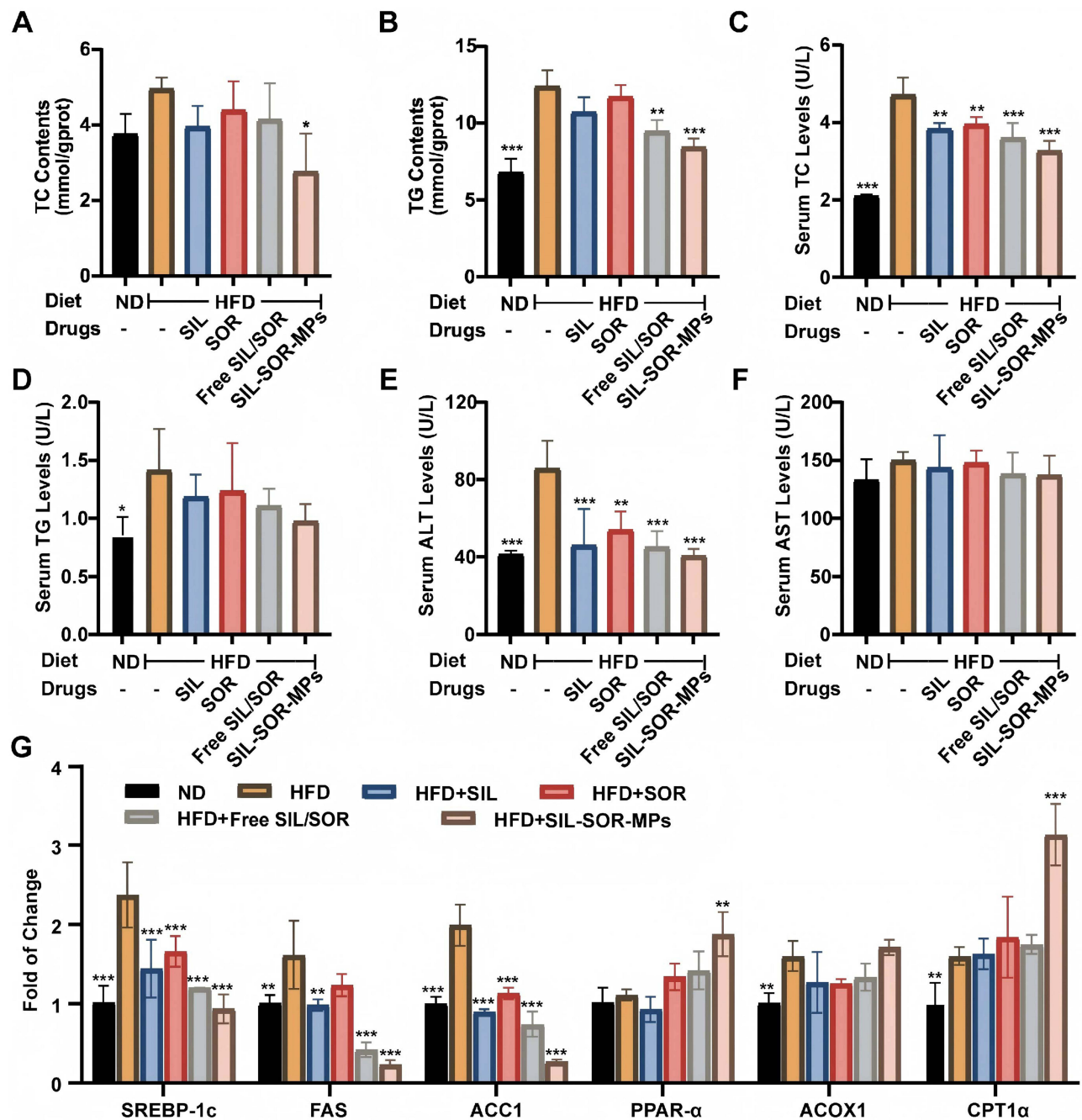


Figure 5 Regulatory effects of SIL-SOR-MPs on lipid metabolism. (A) TC levels in liver tissue across experimental groups. (B) TG levels in liver tissue across experimental groups. (C–F) Serum levels of TC, TG, ALT and AST in each experimental group. (G) Quantitative analysis of genes expression related to lipid synthesis and oxidation (*SREBP-1c*, *FAS*, *ACC1*, *PPAR-α*, *ACOX1*, *CPT1α*). **p* < 0.05, ***p* < 0.001, ****p* < 0.0001 (HFD vs others).

stress and inflammation, causing hepatocyte injury and fibrosis, which can progress to liver cirrhosis or hepatocellular carcinoma.^{26,27} Thus, reducing hepatic lipid accumulation is critical for preventing the progression of MASLD. While lipid-modulating drugs, such as peroxisome proliferator-activated receptor (*PPAR*) and farnesoid X receptor (*FXR*) agonists are being explored in clinical trials, they are still in early stages of development. Despite some promising results, these drugs have not yet achieved the required hepatic histologic endpoints for FDA approval, and further clinical trials are needed to confirm their long-term safety and efficacy.^{28–31}

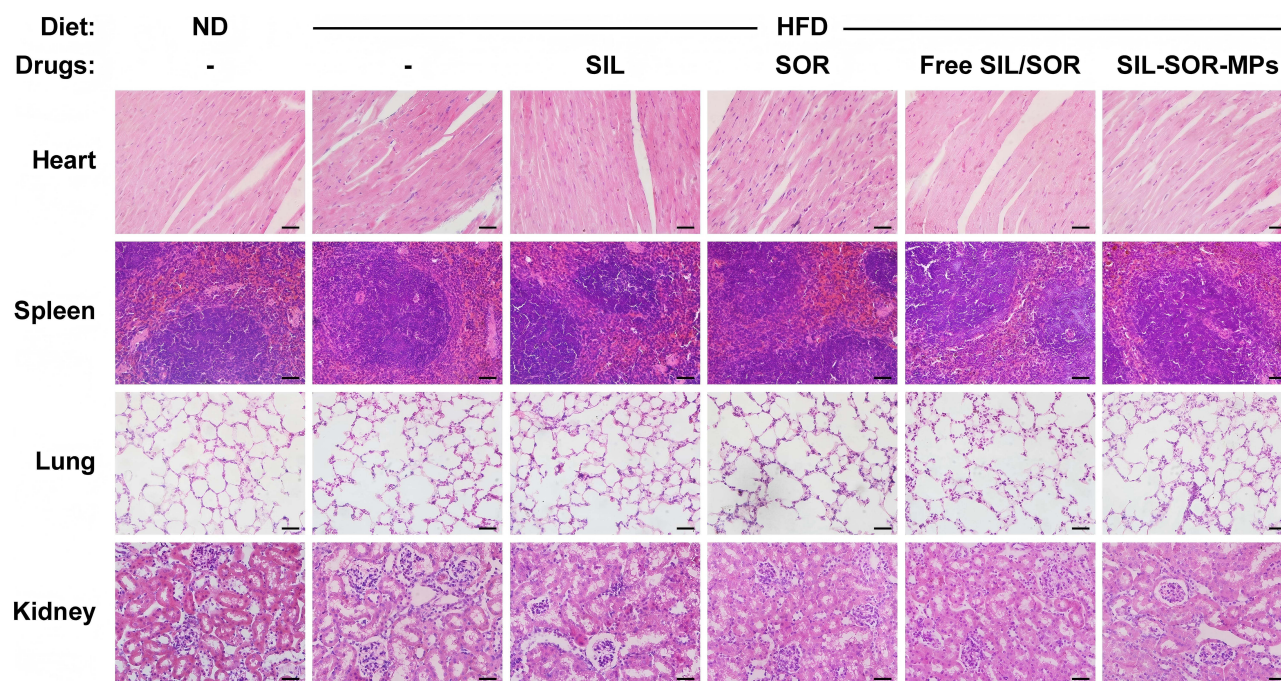


Figure 6 In vivo safety analysis. After 6 weeks of drug treatment, histological analysis of the heart, spleen, lung, and kidney were performed using H&E staining to assess potential toxicity. Scale bar: 20 μ m.

Silibinin, a hepatoprotective agent derived from natural sources, has been widely used in the clinical management of liver disorders.³² Numerous studies have shown that silibinin acts as a potent antioxidant, reducing oxidative stress in the liver and decreasing lipid accumulation. However, its therapeutic potential is limited by poor water solubility and low bioavailability. Sorafenib, a multi-targeted anticancer drug, is the first-line treatment for advanced hepatocellular carcinoma (HCC), though its therapeutic efficacy remains suboptimal.³³ Interesting, at about one-tenth of its clinical dose for HCC, sorafenib has shown beneficial effects on steatosis, inflammation, and fibrosis. Nonetheless, overcoming the high hydrophobicity, low bioavailability, and off-target toxicity of these clinical drugs remains a significant challenge in medical application.

A wide variety of drug delivery systems have been explored for biomedical applications. However, conventional drug carriers often present challenges such as triggering immune responses, causing toxicity, and difficulties in controlling drug release, which hinder the clinical translation of carrier-based nanomedicines.³⁴ In recent years, the integration of nano-delivery and self-assembly technologies has enabled the development of self-delivery drugs.³⁵ In this approach, two or more drugs are self-assembled without the need for excipients through a simple synthesis process, resulting in stable, carrier-free nanomedicines. This strategy has been shown to enhance therapeutic efficacy, reduce drug toxicity, and offer passive targeting to the liver.³⁶ Our study aligns with these findings, demonstrating increased accumulation of nanomedicine in liver tissue, and supporting the potential of silibinin and sorafenib carrier-free microparticles for targeted treatment of MASLD.

In this study, we developed self-assembled silibinin and sorafenib microparticles and investigated their therapeutic potential for MASLD at both cellular and animal levels. In vitro experiments demonstrated that treatment with SIL-SOR-MPs significantly reduced intracellular lipid accumulation in FFA-stimulated cells, indicating a potent lipid-lowering effect. Previous studies have shown that silibinin specifically activates *PPAR- α* and up-regulates *CPT1 α* to promote fatty acid β -oxidation, while concurrently inhibits *SREBP-1c* to reduce fatty acid synthesis.^{37,38} Our qRT-PCR results were consistent with these findings, treatment with SIL-SOR-MPs down-regulated lipogenic gene expression and upregulated genes involved in fatty acid oxidation, supporting the hypothesis that the microparticles modulate lipid metabolism to achieve lipid-lowering effect.

Particle size is known to influence in vivo metabolism and biodistribution. Nanoparticles smaller than 200 nm are typically administered intravenously (i.v.) to exploit the enhanced permeability and retention (EPR) effect and prolong

systemic circulation.³⁹ In contrast, particles larger than 400 nm are rapidly cleared by the mononuclear phagocyte system (MPS) following i.v. administration, limiting their systemic availability.^{40,41} However, larger particles can access the liver directly via the portal circulation when administered intraperitoneally (i.p.), thereby enhancing hepatic targeting. Additionally, the lower protein concentration in the intraperitoneal cavity reduces opsonization by serum proteins, enabling more efficient recognition and uptake by MPS.⁴² Therefore, in our study, SIL-SOR-MPs were administered via i.p. injection, which significantly increased hepatic accumulation and enhanced the bioavailability of both drugs.

Mechanistic studies suggest that silibinin exerts hepatoprotective effects by mitigating mitochondrial dysfunction and oxidative stress through the activation of the AMPK signaling pathway. Meanwhile, low-dose sorafenib induces mitochondrial uncoupling, which subsequently activates AMPK, promoting fatty acid β -oxidation and accelerating lipid catabolism.^{15,43,44} In our in vivo experiments, mice treated with SIL-SOR-MPs exhibited significant reductions in body weight and intrahepatic lipid accumulation compared with those treated with silibinin alone, sorafenib alone or the unformulated free SIL/SOR mixture. These results may be attributed to both the liver-targeted delivery of the micro-particles and the synergistic lipid-lowering effects of the two drugs. The precise molecular mechanisms underlying this synergy will be further investigated in future studies.

Conclusion

In this study, we systematically evaluated the potential of carrier-free silibinin/sorafenib microparticles in the treatment of MASLD. The results showed that the particles significantly ameliorated lipid metabolism abnormalities and attenuated hepatic fat deposition in a MASLD model, and exhibit the effects of inhibiting key genes involved in fatty acid synthesis and promoting key genes related to fatty acid oxidation. This regulatory effect contributed to the restoration of hepatic lipid metabolic homeostasis, yet the precise molecular mechanisms remain incompletely understood. Moreover, the microparticles enhanced the bioavailability of both silibinin and sorafenib, thereby enabling a synergistic therapeutic effect in therapy and improving hepatic efficacy. However, further investigations are required to evaluate the long-term safety profile of the microparticles formulation. In conclusion, the self-assembled carrier-free silibinin/sorafenib microparticles may represent a promising therapeutic strategy for the improving of MASLD treatment.

Acknowledgments

This work was financially supported by the Natural Science Foundation of Hubei Province (2024AFB941), the Research Fund of Jiangnan University (Grant No.2021jczx-002), Research Fund of Department of Education of Hubei Province (Grant No.Q20234409).

Disclosure

The authors declare that they have no known competing financial interests or personal relationships that could have appeared to influence the work reported in this paper.

References

1. Rinella ME, Sookoian S. From NAFLD to MASLD: updated naming and diagnosis criteria for fatty liver disease. *J Lipid Res.* **2024**;65(1):100485. doi:10.1016/j.jlr.2023.100485
2. Wong VW, Ekstedt M, Wong GL, Hagström H. Changing epidemiology, global trends and implications for outcomes of NAFLD. *J Hepatol.* **2023**;79(3):842–852. doi:10.1016/j.jhep.2023.04.036
3. Younossi ZM. Non-alcoholic fatty liver disease - A global public health perspective. *J Hepatol.* **2019**;70(3):531–544. doi:10.1016/j.jhep.2018.10.033
4. Hardy T, Oakley F, Anstee QM, Day CP. Nonalcoholic Fatty Liver Disease: pathogenesis and Disease Spectrum. *Annu Rev Pathol.* **2016**;11(1):451–496. doi:10.1146/annurev-pathol-012615-044224
5. Byrne CD, Targher G. NAFLD: a multisystem disease. *J Hepatol.* **2015**;62(1 Suppl):S47–64. doi:10.1016/j.jhep.2014.12.012
6. Buzzetti E, Pinzani M, Tsochatzis EA. The multiple-hit pathogenesis of non-alcoholic fatty liver disease (NAFLD). *Metabolism.* **2016**;65(8):1038–1048. doi:10.1016/j.metabol.2015.12.012
7. Pafili K, Roden M. Nonalcoholic fatty liver disease (NAFLD) from pathogenesis to treatment concepts in humans. *Mol Metab.* **2021**;50:101122. doi:10.1016/j.molmet.2020.101122
8. Nassir F. NAFLD: mechanisms, Treatments, and Biomarkers. *Biomolecules.* **2022**;12(6). doi:10.3390/biom12060824
9. Keam SJ. Resmetirom: first Approval. *Drugs.* **2024**;84(6):729–735. doi:10.1007/s40265-024-02045-0
10. Powell EE, Wong VW, Rinella M. Non-alcoholic fatty liver disease. *Lancet.* **2021**;397(10290):2212–2224. doi:10.1016/S0140-6736(20)32511-3

11. Paternostro R, Trauner M. Current treatment of non-alcoholic fatty liver disease. *J Intern Med.* 2022;292(2):190–204. doi:10.1111/joim.13531
12. Gillessen A, Schmidt HH. Silymarin as Supportive Treatment in Liver Diseases: a Narrative Review. *Adv Ther.* 2020;37(4):1279–1301. doi:10.1007/s12325-020-01251-y
13. Liu Y, Xu W, Zhai T, You J, Chen Y. Silibinin ameliorates hepatic lipid accumulation and oxidative stress in mice with non-alcoholic steatohepatitis by regulating CFLAR-JNK pathway. *Acta Pharm Sin B.* 2019;9(4):745–757. doi:10.1016/j.apsb.2019.02.006
14. Wilhelm S, Carter C, Lynch M, et al. Discovery and development of sorafenib: a multikinase inhibitor for treating cancer. *Nat Rev Drug Discov.* 2006;5(10):835–844. doi:10.1038/nrd2130
15. Jian C, Fu J, Cheng X, et al. Low-Dose Sorafenib Acts as a Mitochondrial Uncoupler and Ameliorates Nonalcoholic Steatohepatitis. *Cell Metab.* 2020;31(5):892–908.e811. doi:10.1016/j.cmet.2020.04.011
16. Moghtadaie A, Mahboobi H, Fatemizadeh S, Kamal MA. Emerging role of nanotechnology in treatment of non-alcoholic fatty liver disease (NAFLD). *Excli J.* 2023;22:946–974. doi:10.17179/excli2023-6420
17. Li G, Sun B, Li Y, Luo C, He Z, Sun J. Small-Molecule Prodrug Nanoassemblies: an Emerging Nanoplatform for Anticancer Drug Delivery. *Small.* 2021;17(52):e2101460. doi:10.1002/sml.202101460
18. Qiao L, Yang H, Gao S, Li L, Fu X, Wei Q. Research progress on self-assembled nanodrug delivery systems. *J Mater Chem B.* 2022;10(12):1908–1922. doi:10.1039/D1TB02470A
19. Kuang Y, Li Z, Chen H, Wang X, Wen Y, Chen J. Advances in self-assembled nanotechnology in tumor therapy. *Colloids Surf B Biointerfaces.* 2024;237:113838. doi:10.1016/j.colsurfb.2024.113838
20. Gómez-Lechón MJ, Donato MT, Martínez-Romero A, Jiménez N, Castell JV, O'Connor JE. A human hepatocellular in vitro model to investigate steatosis. *Chem Biol Interact.* 2007;165(2):106–116. doi:10.1016/j.cbi.2006.11.004
21. Zhu M, Nie G, Meng H, Xia T, Nel A, Zhao Y. Physicochemical properties determine nanomaterial cellular uptake, transport, and fate. *Acc Chem Res.* 2013;46(3):622–631. doi:10.1021/ar300031y
22. Zhou X, Li Y, Li X, et al. Carrier free nanomedicine to reverse anti-apoptosis and elevate endoplasmic reticulum stress for enhanced photodynamic therapy. *Acta Biomater.* 2022;152:507–518. doi:10.1016/j.actbio.2022.08.045
23. Gluchowski NL, Becuwe M, Walther TC, Farese Jr RV. Lipid droplets and liver disease: from basic biology to clinical implications. *Nat Rev Gastroenterol Hepatol.* 2017;14(6):343–355. doi:10.1038/nrgastro.2017.32
24. Ipsen DH, Lykkesfeldt J, Tveden-Nyborg P. Molecular mechanisms of hepatic lipid accumulation in non-alcoholic fatty liver disease. *Cell Mol Life Sci.* 2018;75(18):3313–3327. doi:10.1007/s00018-018-2860-6
25. Lee E, Korf H, Vidal-Puig A. An adipocentric perspective on the development and progression of non-alcoholic fatty liver disease. *J Hepatol.* 2023;78(5):1048–1062. doi:10.1016/j.jhep.2023.01.024
26. Bessone F, Razori MV, Roma MG. Molecular pathways of nonalcoholic fatty liver disease development and progression. *Cell Mol Life Sci.* 2019;76(1):99–128. doi:10.1007/s00018-018-2947-0
27. Kumar S, Duan Q, Wu R, Harris EN, Su Q. Pathophysiological communication between hepatocytes and non-parenchymal cells in liver injury from NAFLD to liver fibrosis. *Adv Drug Deliv Rev.* 2021;176:113869. doi:10.1016/j.addr.2021.113869
28. Samuel VT, Shulman GI. Nonalcoholic Fatty Liver Disease as a Nexus of Metabolic and Hepatic Diseases. *Cell Metab.* 2018;27(1):22–41. doi:10.1016/j.cmet.2017.08.002
29. Sumida Y, Yoneda M. Current and future pharmacological therapies for NAFLD/NASH. *J Gastroenterol.* 2018;53(3):362–376. doi:10.1007/s00535-017-1415-1
30. Raza S, Rajak S, Upadhyay A, Tewari A, Anthony Sinha R. Current treatment paradigms and emerging therapies for NAFLD/NASH. *Front Biosci.* 2021;26(2):206–237. doi:10.2741/4892
31. Jaffar HM, Al-Asmari F, Khan FA, Rahim MA, Zongo ES. Unveiling its pharmacological spectrum and therapeutic potential in liver diseases-A comprehensive narrative review. *Food Sci Nutr.* 2024;12(5):3097–3111. doi:10.1002/fsn3.4010
32. Rini BI. Sorafenib. *Expert Opin Pharmacother.* 2006;7(4):453–461. doi:10.1517/14656566.7.4.453
33. An J, Zhang Z, Zhang J, Zhang L, Liang G. Research progress in tumor therapy of carrier-free nanodrug. *Biomed Pharmacother.* 2024;178:117258. doi:10.1016/j.biopha.2024.117258
34. Fu S, Li G, Zang W, Zhou X, Shi K, Zhai Y. Pure drug nano-assemblies: a facile carrier-free nanoplatform for efficient cancer therapy. *Acta Pharm Sin B.* 2022;12(1):92–106. doi:10.1016/j.apsb.2021.08.012
35. He Y, Wang Y, Wang L, Jiang W, Wilhelm S. Understanding nanoparticle-liver interactions in nanomedicine. *Expert Opin Drug Deliv.* 2024;21(6):829–843. doi:10.1080/17425247.2024.2375400
36. Vecchione G, Grasselli E, Voci A, et al. Silybin counteracts lipid excess and oxidative stress in cultured steatotic hepatic cells. *World J Gastroenterol.* 2016;22(26):6016–6026. doi:10.3748/wjg.v22.i26.6016
37. Sun R, Xu D, Wei Q, et al. Silybin ameliorates hepatic lipid accumulation and modulates global metabolism in an NAFLD mouse model. *Biomed Pharmacother.* 2020;123:109721. doi:10.1016/j.biopha.2019.109721
38. Blanco E, Shen H, Ferrari M. Principles of nanoparticle design for overcoming biological barriers to drug delivery. *Nature Biotechnol.* 2015;33(9):941–951. doi:10.1038/nbt.3330
39. Pan S, Yuan HY, Zhai QY, et al. The journey of nanoparticles in the abdominal cavity: exploring their in vivo fate and impact factors. *J Control Release.* 2024;376:266–285. doi:10.1016/j.jconrel.2024.10.011
40. Ngo W, Ahmed S, Blackadar C, et al. Why nanoparticles prefer liver macrophage cell uptake in vivo. *Adv Drug Delivery Rev.* 2022;185:1.
41. Petros RA, DeSimone JM. Strategies in the design of nanoparticles for therapeutic applications. *Nat Rev Drug Discov.* 2010;9(8):615–627. doi:10.1038/nrd2591
42. Salomone F, Barbagallo I, Godos J, et al. Silibinin Restores NAD⁺ Levels and Induces the SIRT1/AMPK Pathway in Non-Alcoholic Fatty Liver. *Nutrients.* 2017;9(10):1086. doi:10.3390/nu9101086
43. Liu G, Kuang S, Cao R, Wang J, Peng Q, Sun C. Sorafenib kills liver cancer cells by disrupting SCD1-mediated synthesis of monounsaturated fatty acids via the ATP-AMPK-mTOR-SREBP1 signaling pathway. *FASEB J.* 2019;33(9):10089–10103. doi:10.1096/fj.201802619RR
44. Lazarus JV, Mark HE, Villota-Rivas M, et al. The global NAFLD policy review and preparedness index: are countries ready to address this silent public health challenge? *J Hepatol.* 2022;76(4):771–780. doi:10.1016/j.jhep.2021.10.025

International Journal of Nanomedicine

Dovepress
Taylor & Francis Group

Publish your work in this journal

The International Journal of Nanomedicine is an international, peer-reviewed journal focusing on the application of nanotechnology in diagnostics, therapeutics, and drug delivery systems throughout the biomedical field. This journal is indexed on PubMed Central, MedLine, CAS, SciSearch®, Current Contents®/Clinical Medicine, Journal Citation Reports/Science Edition, EMBase, Scopus and the Elsevier Bibliographic databases. The manuscript management system is completely online and includes a very quick and fair peer-review system, which is all easy to use. Visit <http://www.dovepress.com/testimonials.php> to read real quotes from published authors.

Submit your manuscript here: <https://www.dovepress.com/international-journal-of-nanomedicine-journal>